Geophysical Research Letters

RESEARCH LETTER
10.1029/2019GL082947

A Spring Barrier for Regional Predictions of Summer Arctic Sea Ice

D. B. Bonan[1], M. Bushuk[2], and M. Winton[2]

[1]Department of Atmospheric Sciences, University of Washington, Seattle, WA, USA, [2]Geophysical Fluid Dynamics Laboratory, National Oceanic and Atmospheric Administration, Princeton, NJ, USA

Key Points:
- Sea ice volume is a skillful linear predictor for summer sea ice area in the Arctic and accounts for most of the summer prediction skill
- Nearly all CMIP5 models exhibit a spring predictability barrier for summer sea ice in the marginal seas of the Arctic basin
- Sea ice forecasts for these regions that are initialized prior to 1 June will have substantially less skill than forecasts initialized afterward

Supporting Information:
- Supporting Information S1

Correspondence to:
D. B. Bonan,
dbonan@uw.edu

Citation:
Bonan, D. B., Bushuk, M., & Winton, M. (2019). A spring barrier for regional predictions of summer Arctic sea ice. *Geophysical Research Letters*, *46*, 5937–5947. https://doi.org/10.1029/2019GL082947

Received 21 MAR 2019
Accepted 15 MAY 2019
Accepted article online 20 MAY 2019
Published online 9 JUN 2019

Abstract Seasonal forecast systems can skillfully predict summer Arctic sea ice up to 4 months in advance. For some regions, however, there is a springtime predictability barrier that causes forecasts initialized prior to May to be less skillful. Since this barrier has only been documented in a few general circulation models (GCMs), we evaluate GCMs participating in phase 5 of the Coupled Model Intercomparison Project. We first show sea ice volume skillfully predicts summer sea ice area (SIA) and has similar skill to a perfect model experiment. Given this result, we assess regional SIA predictability across each GCM and find a universal predictability barrier in late spring. For SIA at each summer target month in the marginal seas of the Arctic basin, a notable drop in prediction skill occurs from June to May in each GCM. This suggests summer sea ice forecasts initialized after 1 June will have substantially better prediction skill than forecasts initialized before.

Plain Language Summary A central goal of the sea ice community is to assess the ability of global climate models to accurately predict Arctic sea ice since regional forecasts are a pressing commodity for a broad range of stakeholders. Previous studies assessing sea ice prediction skill suggest that some regions in the Arctic have a "prediction skill barrier" in the spring season, where forecasts of summer sea ice made prior to May are substantially less accurate than forecasts made after May. However, this barrier has only been documented in a few global climate models. In this study, we employ a simple model that uses sea ice volume to predict summer sea ice area. After showing that this simple model reliably predicts regional Arctic sea ice area in the summertime, we test for this barrier across a range of global climate models and find that a spring predictability barrier exists across nearly all global climate models. This suggests that there may be a fundamental limit on skillful predictions of summer Arctic sea ice at regional scales, where forecasts made prior to 1 June will be substantially less accurate than forecasts made after 1 June.

1. Introduction

The Arctic has undergone substantial changes over the last few decades. Near-surface air temperatures have risen at approximately twice the rate of the global mean (Hansen et al., 2010). In terms of sea ice, studies show a sharp decline in its summertime coverage (Cavalieri & Parkinson, 2012; Comiso, 2002; Comiso et al., 2008; Parkinson et al., 1999; Serreze et al., 2007; Stroeve et al., 2007) and thinning across all months (Kwok & Rothrock, 2009; Rothrock et al., 1999). Studies also show a significant loss of multiyear sea ice (Johannessen et al., 1999; Maslanik et al., 2011; Rigor & Wallace, 2004), owing, in part, to a lengthening of the melt season (Perovich & Polashenski, 2012; Stroeve, Markus, et al., 2014). Though most of these changes are striking emblems of anthropogenic climate change, they have also fueled considerable interest in the predictability of Arctic sea ice on seasonal to interannual time scales (e.g., Eicken, 2013; Jung et al., 2016). Given the fundamental role that sea ice plays in the climate system, terrestrial and marine ecosystems, and human population, skillful forecasts of Arctic sea ice are valuable to a broad range of stakeholders (e.g., Ford & Smit, 2004; Jung et al., 2016; Laliberté et al., 2016; Melia et al., 2016; Pizzolato et al., 2016; Regehr et al., 2007; Smith & Stephenson, 2013; Wyllie-Echeverria & Wooster, 1998).

A recent goal of the sea ice community is to assess the predictability and prediction skill of Arctic sea ice. Considerable effort has gone toward developing both statistical and dynamical sea ice prediction systems. Numerous studies using fully coupled general circulation models (GCMs) have quantified the seasonal prediction skill of pan-Arctic sea ice extent (SIE), for example, by performing suites of initialized retrospective

forecasts, also known as hindcasts. These studies have found forecast skill for detrended pan-Arctic SIE at lead times of 1–6 months (e.g., Blanchard-Wrigglesworth et al., 2015; Bushuk et al., 2017a; Chevallier et al., 2013; Guemas et al., 2016; Merryfield et al., 2013; Msadek et al., 2014; Peterson et al., 2015; Sigmond et al., 2013; Wang et al., 2013). Similarly, statistical models also show detrended pan-Arctic SIE prediction skill, with significance at lead times of up to 6 months (Lindsay et al., 2008; Petty et al., 2017; Schröder et al., 2014; Stroeve, Hamilton, et al., 2014; Wang et al., 2016; Williams et al., 2016; Yuan et al., 2016).

Complementing these GCM-based hindcast prediction assessments and statistical models is a number of "perfect model" (PM) studies, which assess the predictability of a particular GCM in the case of perfectly known initial conditions and no underlying model physics uncertainties. The only source of forecast error in PM experiments is the chaotic growth associated with small initial condition errors; such an approach provides guidance on the upper limits of predictability by asking how well a particular model can predict itself (e.g., Collins, 2002). Previous PM studies have shown that the potential predictability for pan-Arctic SIE remains statistically significant at lead times up to 1–2 years (Blanchard-Wrigglesworth & Bushuk, 2018; Blanchard-Wrigglesworth, Bitz, et al., 2011; Bushuk et al., 2018; Day et al., 2016; Germe et al., 2014; Holland et al., 2011; Koenigk & Mikolajewicz, 2009; Tietsche et al., 2014), which is considerably longer than that of GCM-based initialized forecasts.

While these studies have provided an important first step in assessing the ability of fully coupled GCMs to predict Arctic sea ice, the utility is somewhat limited for the aforementioned stakeholders. Arguably, knowledge of regional sea ice predictability is of greater economic, ecological, and climatic consequences. Given its value, studies have begun to establish important baselines for regional Arctic SIE prediction skill using dynamical forecast systems. For instance, Day, Tietsche, and Hawkins (2014) use PM experiments performed with HadGEM1.2 and find the seasonal ice zones of the North Atlantic have significant SIE predictability at lead times of 1–2 years. Similarly, Sigmond et al. (2016) demonstrate predictions of regional ice advance and retreat dates are particularly skillful for areas such as Hudson Bay, Baffin Bay, Labrador Sea, and Chukchi Sea. Krikken et al. (2016) find skill for sea ice forecasts at up to 6-month lead times for the Barents Sea, Kara Sea, and the Northeast passage region. By performing multiple hindcast simulations using a fully coupled GCM, Bushuk et al. (2017a) provide the first extensive analysis of regional Arctic SIE prediction skill, highlighting both key physical mechanisms underlying skillful predictions and assessing forecast skill in each region. Consistent with previous work that relates summer sea ice prediction skill to sea ice thickness (Blanchard-Wrigglesworth, Armour, et al., 2011; Chevallier & Salas-Mélia, 2012; Collow et al., 2015; Day, Hawkins, et al., 2014; Dirkson et al., 2017), Bushuk et al. (2017a) demonstrate that skillful regional predictions of summertime sea ice depend on initialization of sea ice thickness, while wintertime predictions hinge on initialization of subsurface ocean temperatures.

Additionally, Bushuk et al. (2017a) find that the East Siberian, Laptev, and Beaufort Seas each display a sharp drop in SIE prediction skill in either May or June for all summer target months. Day, Tietsche, and Hawkins (2014) also identify a drop in prediction skill in May but for pan-Arctic SIE. In their work, PM forecasts initialized in May are found to lose skill more quickly than forecasts initialized in July. More recently, Brunette et al. (2019) present an observational-based statistical forecast model which uses winter coastal divergence as a predictor of summer minimum SIE in the Laptev Sea. They find maximal skill when considering coastal divergence up to the first week of May and report a drop in skill when the divergence is compared to the first week of April, consistent with a spring predictability barrier. This spring prediction skill barrier has also been shown to exist across the East Siberian, Laptev, and Beaufort Seas in PM experiments (e.g., Bushuk et al., 2018), which suggests there may be a fundamental limit on regional summer sea ice forecasts. Yet, beyond these studies, this springtime predictability barrier has not yet been quantified or examined in further detail. Though it has been noted in a few GCMs, a key question that remains unanswered is the following: Does this spring predictability barrier exist across other GCMs? Answering this question is critical for quantifying the potential ability of GCMs to make accurate predictions of regional Arctic sea ice. Indeed, if this barrier does exist, a crucial related question is the following: What date should forecasts be initialized for accurate predictions of summer Arctic sea ice? As the Arctic undergoes change and ocean regions become ice free, summertime sea ice predictions may prove to be a more pressing commodity. Knowing exactly when to initialize GCMs will prove to be key for providing accurate sea ice forecasts.

Motivated by these questions, we test for the existence of this springtime predictability barrier across other GCMs by using output from phase 5 of the Coupled Model Intercomparison Project (CMIP5). In what fol-

lows, we first use a fully coupled GCM to show sea ice volume (SIV) accurately predicts sea ice area (SIA) at different summertime target months by comparing their lead-time correlations to a skill metric from a set of PM experiments. This comparison shows that SIV is the dominant source of predictability for summer SIA and captures the springtime prediction skill barrier. We then use this simple linear regression model to assess SIA prediction skill for the ensemble of GCMs participating in CMIP5. After identifying the regional SIA predictability across the GCMs, we characterize both the magnitude and temporal structure of SIA prediction skill and discuss implications of these results.

2. Methodology

2.1. CMIP5 Output

We use monthly output from the preindustrial control runs of 38 different GCMs (see supporting information Table S1) participating in CMIP5 (Taylor et al., 2012). While the preindustrial control simulations have different regional Arctic sea ice concentration compared to the present day, the simulations are not influenced by anthropogenic changes, which allows us to study Arctic sea ice predictability over long time periods using variability unique to a constant climate. We consider two quantities for this study: sea ice concentration and sea ice thickness. The set of GCMs evaluated for both quantities reflect those that provide the necessary output (see Table S1). All model output is interpolated to a common $1° \times 1°$ analysis grid using nearest-neighbor interpolation. Since regridding can result in differences from the native grid (Hofstra et al., 2008), we compare regional SIA and SIV computed on each grid and find little difference between the two. We analyze the last 200 years of each preindustrial control simulation to account for model spin up and for consistency across the GCMs (see Table S1 for model years). With each GCM, we compute SIA and SIV for pan-Arctic and 14 Arctic regions following the domains used by Day, Tietsche, and Hawkins (2014) and Bushuk et al. (2017a; see Figure S1).

2.2. GFDL-FLOR Output

Since PM experiments were not performed across CMIP5, we cannot directly assess the maximum SIA prediction skill of each GCM. To circumvent this problem, we make use of two experiment suites performed using the same GCM, which allows us to assess the ability of SIV to accurately predict SIA (two quantities that can be calculated from the CMIP5 output). We use two experiments described in Bushuk et al. (2018): a 300-year control run and a set of PM experiments performed using the Geophysical Fluid Dynamics Laboratory (GFDL) Forecast-oriented Low Ocean Resolution (FLOR) climate model (Vecchi et al., 2014). Both the control run and PM experiments use radiative forcing and land use conditions that are representative of 1990. We also use a 300-year control run that uses radiative forcing and land use conditions representative of 1860 to compare sea ice predictability in different time periods. The PM experiments branch from the 300-year 1990 control integration of GFDL-FLOR using six different years and six start dates for each year (1 January, 1 March, 1 May, 1 July, 1 September, and 1 November). Each start date contains 12 ensemble members that are initialized with a random spatially uncorrelated Gaussian perturbation (with standard deviation 10^{-4} K) to the sea surface temperature (SST) field and then run forward in time for 3 years. Output from each control integration is interpolated to a common $1° \times 1°$ analysis grid using the nearest-neighbor algorithm and is then used to compute SIA and SIV for pan-Arctic and 14 regional Arctic domains (see Figure S1).

2.3. Predictability Skill Metrics

To assess the ability of SIV to accurately predict SIA, we compare the skill identified using the PM experiments to the correlation coefficients of SIV at different lead times and SIA at different target months. Following Bushuk et al. (2018), we assess SIA prediction skill of the PM experiments by using the unbiased anomaly correlation coefficient (ACC), which is a modified ACC definition designed to reduce biases associated with start date sampling that arise when using the standard definition of PM ACC of Collins (2002). The unbiased ACC is defined as the square root of the mean squared-error skill score. The mean squared-error skill score is computed by letting each ensemble member take a turn as a synthetic "truth" member and using the ensemble mean of the remaining $N - 1$ members to predict this truth member (see Bushuk et al., 2018). PM ACC values for even initialization months (1 February, 1 April, 1 June, 1 August, 1 October, and 1 December) are obtained by linearly interpolating the skill values obtained for odd initialization months, following the procedure used in Bushuk et al. (2018). PM ACC values near one indicate high prediction skill and values closer to zero indicate little-to-no prediction skill.

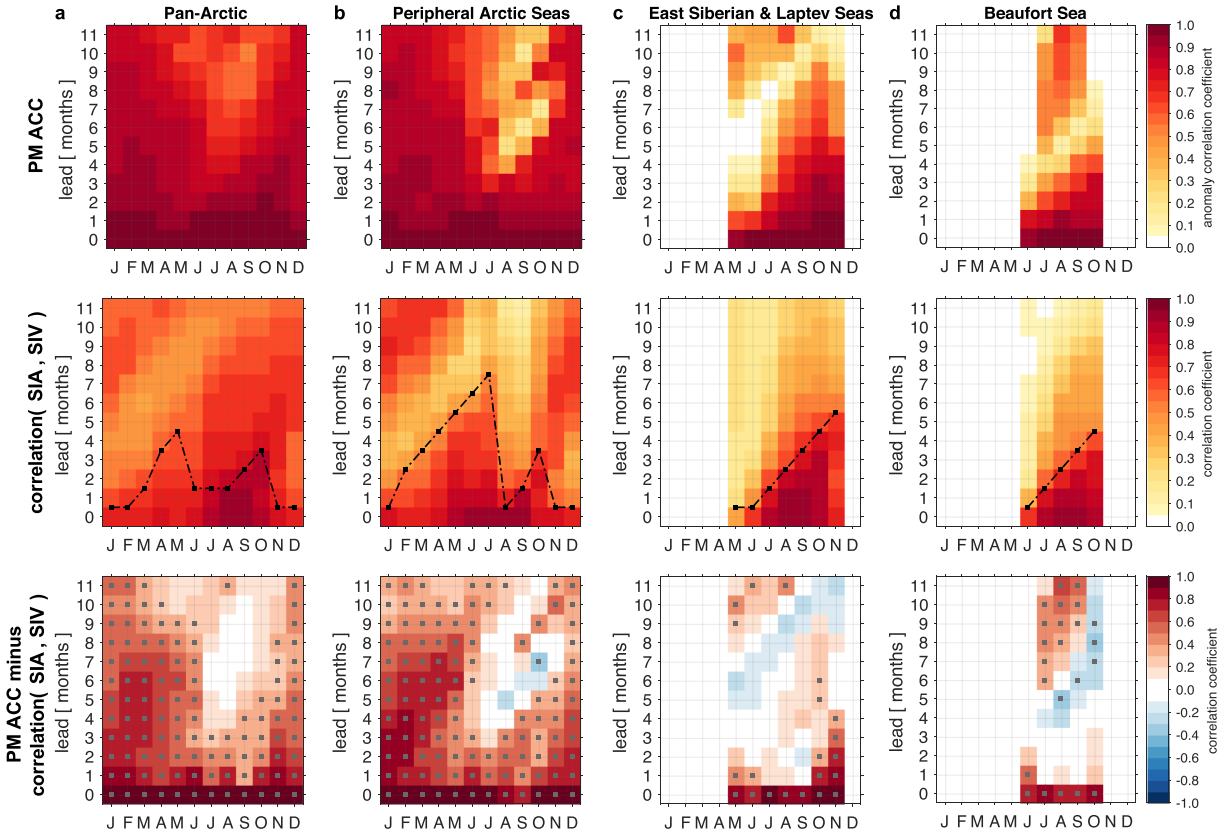

Figure 1. Seasonal sea ice area (SIA) prediction skill from Geophysical Fluid Dynamics Laboratory Forecast-oriented Low Ocean Resolution climate model for (a) pan-Arctic, (b) the Peripheral Arctic Seas, (c) the East Siberian and Laptev Seas, and (d) the Beaufort Sea determined by the perfect model (PM) anomaly correlation coefficient (ACC) values from a set of PM experiments and when using sea ice volume (SIV) as a predictor of SIA. PM ACC values greater than 0.20 are significant at the 95% confidence level based on a *t* test. All correlations in the middle panels exceeding 0.16 are significant at the 95% confidence level based on a *t* test accounting for autocorrelation. The black line in the middle panels indicates the largest decorrelation between two lead months for each target month. The difference between the PM ACC values and SIV and SIA Pearson correlation coefficients is computed using the Fisher's *z*-transformation and is shown in the bottom set of panels. Gray squares indicate significant differences at the 95% confidence level. Values are plotted as a function of target month and forecast lead time and are only plotted for target months with SIA standard deviation greater than 0.03×10^6 km^2 in the Geophysical Fluid Dynamics Laboratory Forecast-oriented Low Ocean Resolution climate model control run with radiative forcing and land use changes representative of 1990.

3. SIV Skillfully Predicts Summer SIA

The lack of PM experiments across a wide range of GCMs means we must find another way to assess SIA predictability within CMIP5. Since previous work suggests that SIV is an important source of predictability for summer SIA (Blanchard-Wrigglesworth et al., 2017; Blanchard-Wrigglesworth, Armour, et al., 2011; Blockley & Peterson, 2018; Bushuk et al., 2017a, 2017b; Collow et al., 2015; Day, Hawkins, et al., 2014; Holland et al., 2011) and there is an abundance of sea ice concentration and sea ice thickness output from GCMs participating in CMIP5, it is possible SIA and SIV can be used to assess Arctic sea ice prediction skill across the GCMs. To evaluate the efficacy of SIV as a predictor of SIA, we first assess the ability of SIV anomalies at different lead months to skillfully predict SIA anomalies at different target months. To carry out this assessment, we compare the PM ACC skill identified by the GFDL-FLOR PM experiments to the correlation coefficients of monthly SIV and SIA computed from the GFDL-FLOR 1990 control run. We compute correlations between regional SIA and earlier SIV at lead times up to 11 months. Since the PM experiments are initialized on the first of each month, we compute 2-month averages of SIV to create a first-of-the-month SIV time series, which facilitates a clean comparison with the PM experiments. Correlations of SIV and SIA computed using monthly centered time series produce similar results but are more difficult to compare with the PM experiments. It is worth noting that the 2-month averages give an approximate first-of-the-month SIV time series. Thus, any correlation between SIV and SIA shows the ability of SIV initialized approximately on the first-of-the-month to predict monthly averaged SIA.

Figure 1 shows the PM ACC values for SIA, correlation coefficients of previous monthly SIV with monthly SIA, and their difference for four area domains: the pan-Arctic, the Peripheral Arctic Seas, the East Siberian and Laptev Seas, and the Beaufort Sea. We choose these regions based on previous work assessing sea ice prediction skill in GFDL-FLOR, which showed the spring predictability barrier exists in the East Siberian, Laptev, and Beaufort Seas. Additionally, we choose to show the pan-Arctic and the Peripheral Arctic Seas—which encompasses the Greenland, Iceland, and Norwegian Seas, Barents Sea, Bering Sea, Sea of Okhotsk, and Hudson Bay (see Figure S1)—to illustrate the different predictability structures governing SIA. The difference between the PM ACC values and SIV and SIA correlation coefficients is computed using the Fisher's z-transformation (Meng et al., 1992), which allows the correlation values to become normally distributed and thus directly compared.

When considering SIV as a predictor of pan-Arctic SIA (Figure 1a), we find that for winter target months, a considerable amount of skill identified by the PM ACC values is not captured. The PM ACC values all show high correlation values (>0.8) at lead times of up to 11 months, whereas the correlation coefficients of pan-Arctic SIV and pan-Arctic SIA are much lower, leaving significantly large differences in the wintertime (squares denote statistically significant differences at the 95% confidence level). Conversely, in the summertime, SIV acts as a better predictor of SIA, capturing more—though not all—of the PM ACC skill (Figure 1a). These results are consistent with predictions of summer SIA depending on previous sea ice thickness and wintertime SIA predictions depending on other sources of predictability, such as upper ocean heat content (Bushuk et al., 2017a). For regions of seasonal ice cover (i.e., Peripheral Arctic Seas), the results are similar: SIV can explain some of the summertime SIA variance and little of the wintertime SIA variance (Figure 1b). This result is again consistent with upper ocean heat content being a better wintertime SIA predictor. For sea ice in the Peripheral Arctic Seas and pan-Arctic, we find no clear indication of a springtime prediction skill barrier; there is no consistent month of maximal correlation drop-off across target months (see black line). While these correlation values display some diagonal structure, the diagonal features are less prominently defined across a single initialization month.

For the East Siberian and Laptev Seas (Figure 1c)—two regions where the spring predictability barrier was first identified—we find SIV skillfully predicts summertime SIA. The PM ACC values show a skill barrier, where at lead times corresponding to May, there is a significant drop-off in prediction skill of approximately 0.3–0.4 (Figure 1c). By computing the maximal decorrelation across all target months (see black line), we find this barrier also exists when using SIV to predict SIA in the East Siberian and Laptev Seas (Figure 1c). Note during the wintertime, this region is fully ice covered, hence the zero correlations (i.e., white space) in the winter months. Comparing the PM ACC skill to the SIV and SIA correlations, we find the correlations capture this skill barrier across all target months with nearly all correlation coefficient differences being statistically insignificant and falling below ~0.1. However, the large positive correlations values leftover at the growth seasons (see November target months of Figure 1c) indicates that there are other sources of SIA prediction skill, which is consistent with ocean temperatures playing a role for SIA predictability in the ice growth season (Blanchard-Wrigglesworth, Bitz, et al., 2011). Additionally, the large differences at lead zero are consistent with SIA prediction skill resulting from SIA persistence and some atmospheric predictability on submonthly time scales.

For the Beaufort Sea, we find similar results: SIV acts as a skillful linear predictor of summertime SIA (Figure 1d). The SIV and SIA correlations explain most of the PM ACC values and capture the prediction skill barrier. Indeed, the correlations miss the magnitude of PM ACC skill at both the beginning and end of the summer season and at lead zero, which again suggests there are other sources of skill on submonthly time scales and at seasonal transitions. Yet, even with these differences, the majority of the PM ACC values can be explained when using SIV to predict SIA in the summertime. This suggests that SIV is the dominant source of predictability for summer SIA in the Arctic and that SIV acts as a skillful linear predictor of summer SIA—which is consistent with the results from Ordoñez et al. (2018). Most importantly for the present study, the comparison associates the spring predictability barrier with the decorrelation of SIA and SIV, which allows us to employ this regression model to test for the barrier across the free-running GCM preindustrial control experiments available from the CMIP5 archive.

4. A Springtime Predictability Barrier Across CMIP5

We next apply the simple linear regression model to the CMIP5 ensemble. To do this, we correlate SIA at January through December target months with SIV at lead times up to 11 months over the 200-year

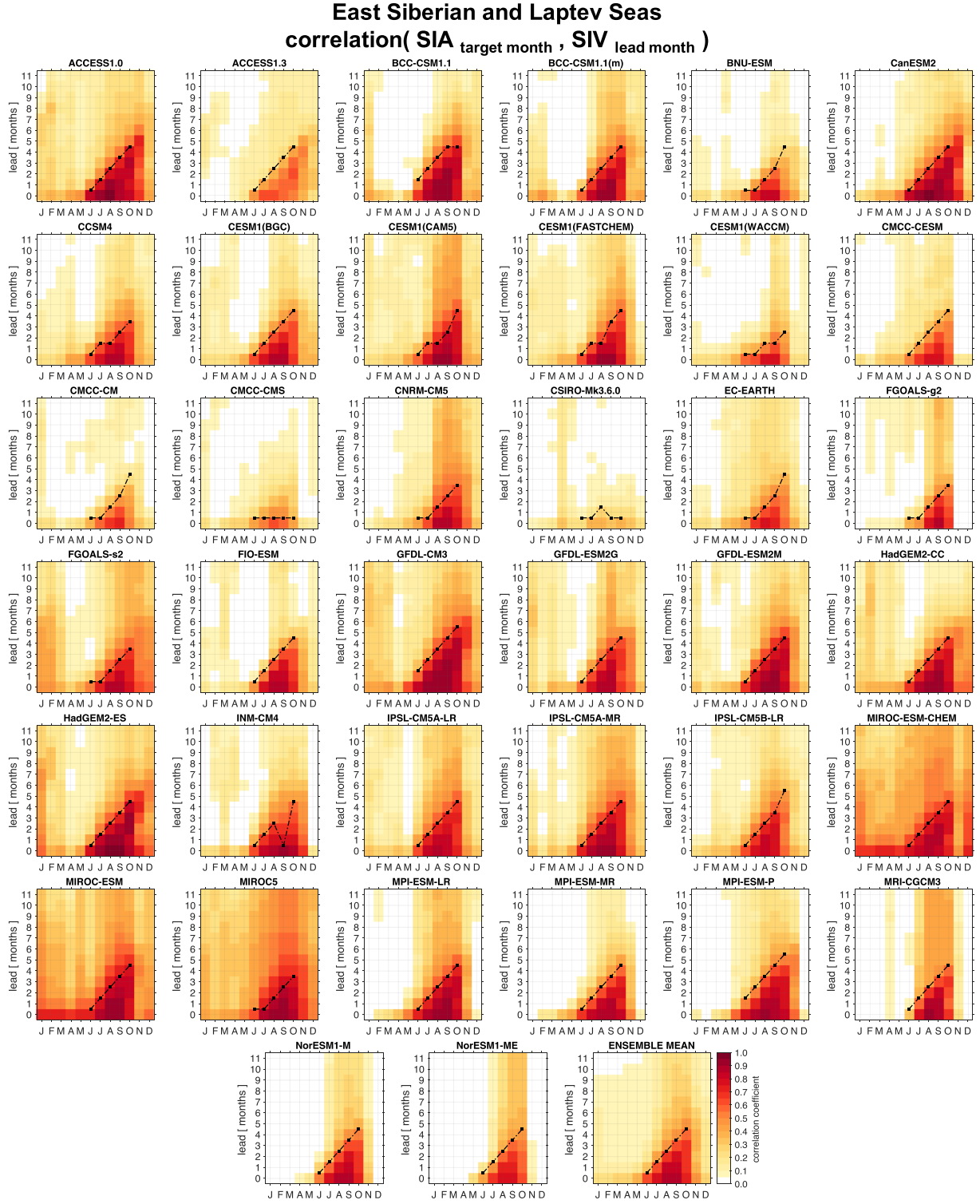

Figure 2. Pearson correlation coefficient of sea ice area (SIA) at January through December target months with sea ice volume (SIV) at lead times up to 11 months in the East Siberian and Laptev Seas. Correlation values are shown for the pre-inudstrial control simulations of 38 fully coupled general circulation models based on a 200-year time series. The ensemble mean correlation structure for all general circulation models is shown in the last panel. All correlations exceeding 0.18 are significant at the 95% confidence level based on a *t* test accounting for autocorrelation. The black line in each panel indicates the largest decorrelation between two lead months for summer target months (June–October).

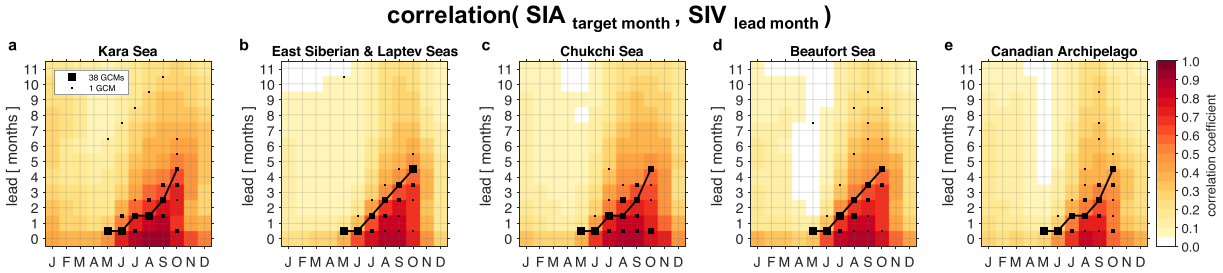

Figure 3. Pearson correlation coefficient of sea ice area (SIA) at January through December target months with sea ice volume (SIV) at lead times of 0 to 11 months in the (a) Kara Sea, (b) East Siberian and Laptev Seas, (c) Chukchi Sea, (d) Beaufort Sea, and (e) Canadian Archipelago. Correlation values are based on a 200-year time series from preindustrial control simulations and are shown for the ensemble mean of 38 general circulation models (GCMs). The black squares in each panel denote the largest decorrelation between two lead months for May through October target months, where the square size indicates the number of GCMs that decorrelate at that lead time. The largest square corresponds to 38 GCMs, and the smallest square corresponds to one GCM. The black line is when most GCMs decorrelate.

time period in each regional domain. Doing this for each GCM allows us to assess SIA predictability across the ensemble of GCMs. Again, before correlations are computed, we average SIV over 2 months, creating a first-of-the-month SIV time series that quantifies the ability of SIV initialized on the first of each month to predict monthly averaged SIA. Here lead zero is the correlation of monthly centered SIA and first-of-the-month SIV.

Figure 2 shows the correlation structure that emerges for all 38 fully coupled GCMs and the multimodel ensemble mean when considering SIA in the East Siberian and Laptev Seas (see Figure S1). Though many of the GCMs have different sea ice components and model biases (Massonnet et al., 2012), nearly all GCMs show a remarkably universal decorrelation structure. Across the GCMs, we find there is a consistent and significant drop-off in correlation corresponding to SIV in May or June. At each May or June lead time, correlation coefficients drop-off by approximately 0.2–0.3 (see Figure S4). To show the tendency of each GCM to decorrelate at the same initialization month regardless of the SIA target month, we compute the months of the largest decorrelation for the summer season (June–October). Correlations are overall lower for November–April target months since most regions are fully ice covered and have little SIA variance (see Figure S3). The black line in each plot represents the months of largest decorrelation and thus a predictability barrier. The months of largest decorrelation for the majority of the GCMs (~24) occurs when SIV transitions from 1 June to 1 May. Indeed, there is some intermodel spread in the timing of decorrelation. For instance, the largest decorrelation for some GCMs (e.g., BNU-ESM, CCSM4, CESM1(WACCM), CMCC-CM, EC-EARTH, FGOALS-g2, and FGOALS-s2) occurs at both May to April SIV transitions and June to May SIV transitions, while others (e.g., CMCC-CMS) show a distinct correlation coefficient structure reminiscent of a barrier but no universal decorrelation time (as indicated by the flat black line). Though there is sizable spread, there is also a tendency for the majority of the models to decorrelate at the same exact initialization time; the months of the largest SIV decorrelation are from 1 June to 1 May in the ensemble mean, which suggests the predictability barrier occurs between 1 June and 1 May.

In addition to intermodel spread in the timing of the barrier, there is also intermodel spread in the magnitude of correlations across GCMs. MIROC-ESM-CHEM, MIROC-ESM, and MIROC5 all show substantially higher correlations at all target months when compared to the rest of the GCMs, which likely indicates spread in PM predictability (e.g., Blanchard-Wrigglesworth & Bushuk, 2018). There is also considerable intermodel variability in seasonal cycles of SIA and SIV (see Figure S2). Yet, despite this spread, each GCM exhibits a spring predictability barrier. While the large intermodel spread in both the timing of decorrelation and magnitude of correlations warrants further work to explain these differences, for the remainder of this analysis, we focus on the nearly universal correlation structure that suggests an inherent spring predictability barrier for regional forecasts of summer Arctic sea ice. Such similar correlation structures across GCMs in the East Siberian and Laptev Seas suggest other regions may have this predictability barrier as well. To examine for this barrier in other regions, we perform the same analysis for each regional domain. Since the majority of our analysis focuses on the CMIP5 preindustrial controls runs—which have considerably different forcing scenarios and land use conditions than the present day—we select regions that have a large magnitude of summer SIA variance (see Figure S3).

Figure 3 shows the correlation coefficient values between SIA at January through December target months and SIV at lead times of 0 to 11 months in the Kara Sea (Figure 3a), East Siberian and Laptev Seas (Figure 3b), Chukchi Sea (Figure 3c), Beaufort Sea (Figure 3d), and Canadian Archipelago (Figure 3e). Since each GCM exhibits a similar correlation coefficient structure, the ensemble mean correlation coefficient structure of all 38 GCMs is shown. Note the ensemble mean correlation pattern is computed using the Fisher's z-transformation (Meng et al., 1992) to allow for the correlation values of each GCM to be normally distributed. When considering the ability of SIV to predict SIA in the Kara Sea (Figure 3a), a distinct correlation structure emerges that shows a consistent late spring decorrelation of SIA and SIV. The black line represents the most common decorrelation time across GCMs. The correlation coefficients drop by ~0.2–0.3 at all May and June SIV lead times (see Figure S4). To quantify the intermodel spread in the correlation patterns, we also calculate the months of the largest decorrelation between summertime SIA target months and SIV lead times for each GCM. The square in Figure 3 indicates the number of GCMs that decorrelate at that specific lead time, with the largest square corresponding to all 38 GCMs and the smallest square denoting a single GCM. For the Kara Sea (Figure 3a), the months of largest decorrelation tend to be from June to May. Though, it is worth noting that there is a fairly equal split between the GCMs that decorrelate from May to April and those that decorrelate from June to May. Similarly, for the East Siberian and Laptev Seas (Figure 3b), Chukchi Sea (Figure 3c), and Beaufort Sea (Figure 3d), we find a distinct diagonal feature of decorrelation. Computing the largest correlation drop-off across GCMs (the black line) suggests the predictability barrier in these regions occurs between 1 June and 1 May. The Beaufort Sea (Figure 3d) has one of the most striking predictability barriers, with the largest drop-off in correlation at each summer target month (~0.3) and a tightly constrained intermodel spread in barrier timing (Figure 3d). For the Canadian Archipelago (Figure 3e)—a region that encompasses the Northwest Passage—there are lower correlations, but there remains a similar barrier structure with significant decorrelation occurring as SIV transitions from 1 June to 1 May. The lower correlations could be a result of how the Canadian Archipelago is represented in these coarse-resolution GCMs, which varies considerably.

5. Discussion and Conclusion

Predictions of Arctic sea ice are needed by a broad range of stakeholders, especially on regional scales (Eicken, 2013; Jung et al., 2016). Previous studies assessing GCM-based forecasts, however, suggest that there may be a predictability barrier in the springtime for sea ice in some Arctic regions (Bushuk et al., 2017a; Day, Tietsche, et al., 2014). Thus, forecasts of summer Arctic sea ice concentration may be less accurate prior to May. Still, this barrier has yet to be fully explored and quantified across an ensemble of GCMs due, in part, to the lack of PM experiments. A simpler framework is needed to assess Arctic sea ice predictability and the robustness of this barrier across GCMs. In this study, we developed such a framework and evaluated seasonal SIA predictability using output from the preindustrial control runs of an ensemble of GCMs participating in CMIP5. By employing a simple linear regression model that uses previous monthly SIV and monthly SIA, we have found that SIV acts as a skillful predictor of summertime SIA and characterizes the summer SIA predictability in a range of regional domains. In these regions, the correlation coefficients of lead-time SIV and target-month SIA are comparable to PM ACC skill estimates—which provide guidance on the maximum available predictability (see Figure 1). A potential caveat to this prediction skill comparison is the use of a single GCM. A useful extension of this line of research would be to compare PM skill in other GCMs with the prediction skill of SIV. This result does indicate, however, that SIV is the dominant source of predictability for summer SIA and suggests that this simple linear regression model can be applied to the entire CMIP5 ensemble to assess summer Arctic sea ice predictability across a larger swath of GCMs.

Despite having considerably different sea ice components (Massonnet et al., 2012) and a large spread of SIV and SIA seasonal cycles (see Figure S2), nearly all of the CMIP5 GCMs display a remarkably similar correlation structure that shows substantial decorrelation as SIV transitions from June to May in the East Siberian and Laptev Seas (see Figure 2). The black lines in each panel correspond to the initialization months that have the largest drop-off in correlation for summer target months (June–October). Though there is some intermodel spread in the timing of decorrelation, there is a tendency for all GCMs to decorrelate at a similar lead time: The month of largest SIV lead time decorrelation for most GCMs is from June to May for all summer target months. This universal decorrelation feature suggests there is a predictability barrier that occurs between the months of June and May. Such similar correlation coefficient structures across GCMs in the East Siberian and Laptev Seas (Figure 2) raises another question: Does this spring predictability barrier

exist in other regions of the Arctic? Figure 3 shows the ensemble mean correlation pattern of all 38 GCMs for the Kara Sea, East Siberian and Laptev Seas, Chukchi Sea, Beaufort Sea, and Canadian Archipelago. In these regions, the structure and magnitude of decorrelation for all summer target months also suggests there is a springtime predictability barrier that occurs between 1 June and 1 May. Indeed, there remains sizable spread in the timing of decorrelation across GCMs (as indicated by the size of the black squares), but there is a tendency for each GCM to maximally decorrelate from June to May (see black line). Perhaps most notably is that these Arctic regions—the marginal seas of the Arctic basin—encompass most of the viable summer shipping routes, which suggests this predictability barrier may limit accurate forecasts for end users.

So how early can models be initialized and still make highly skillful forecasts of summer sea ice? Though we show that this barrier is robust, further experiments with daily temporal resolution are required to pinpoint its precise date. How far into the melt season must GCM-based predictions be initialized in order to avoid the unpredictable effects of atmospheric chaos and melt onset variability? Here, based on a diagnostic regional predictability analysis of CMIP5 GCMs, we suggest that a 1 June initialization is sufficiently past the spring predictability barrier. This suggestion, however, is made using monthly output, which limits the temporal resolution, and thus precise barrier timing. Additionally, the use of preindustrial control simulations may limit constraints on the exact timing of the barrier since some processes, such as melt onset, occur later in the spring when compared to the present-day climate. However, a comparison of a 1990 and 1860 control run in GFDL-FLOR shows that the timing of maximum decorrelation is broadly consistent between the two time periods (see Figure S5), indicating that the barrier timing diagnosed from preindustrial control runs is also relevant for climates similar to the present day. Indeed, the 1990 predictability barrier is sharper and has larger magnitude correlations of SIA and SIV (see Figure S5), which suggests that volume-based summer sea ice predictability may be a function of climate mean state, consistent with the earlier findings of Holland and Stroeve (2011). In addition to quantifying sea ice prediction under a changing climate, future research should address the intermodel variability in SIA prediction skill. MIROC-ESM, MIROC-ESM-CHEM, and MIROC5 all show considerably higher correlations of SIA and SIV when compared to the other GCMs. Understanding why SIV acts as a better SIA predictor with some GCMs and less so with others (e.g., CSIRO-Mk3.6.0) may permit a better quantification of the ability of GCMs to predict Arctic sea ice (e.g., Blanchard-Wrigglesworth & Bushuk, 2018). Perhaps more important, however, is the robustness of this spring predictability barrier, which raises an important question: What physical mechanism is so universal across GCMs? The barrier timing corresponds quite closely with the timing of surface melt onset, which is largely dictated by unpredictable year-to-year atmospheric conditions (Mortin et al., 2016; Stroeve, Markus, et al., 2014). While future work is required to address the processes in the spring that generate a predictability barrier, this suggests that the ice-albedo feedback may be an important contributor.

In the context of operational Arctic sea ice forecasts, our analyses suggest accurate predictions may hinge on better observational data sets that allow for initializations sufficiently past the date of this barrier. Currently, algorithms that derive Arctic sea ice thickness terminate in mid-April since it is difficult to differentiate between sea ice leads and surface melt ponds during the melt season (Ricker et al., 2014; Tilling et al., 2015). The spring predictability barrier identified in this study highlights the critical importance of extending sea ice thickness products as far as possible into the melt season to allow for an observationally constrained initialization of sea ice thickness near 1 June. We hope this study will motivate future work along these lines.

Acknowledgments
This work benefited from illuminating discussions with Kyle Armour, Cecilia Bitz, and Ian Eisenman. We thank Jack Landy for providing guidance on algorithms that estimate Arctic sea ice thickness. We also thank Edward Blanchard-Wrigglesworth, Ben Bronselaer, and Alex Haumann for providing useful comments on a draft of this manuscript. D. B. B. acknowledges support from the NOAA Ernest F. Hollings Scholarship. The CMIP5 data for this study are accessible at the Earth System Grid Federation (ESGF) Portal (https://esgf-node.llnl.gov/search/cmip5/).

References

Blanchard-Wrigglesworth, E., Armour, K. C., Bitz, C. M., & DeWeaver, E. (2011). Persistence and inherent predictability of Arctic sea ice in a GCM ensemble and observations. *Journal of Climate*, *24*(1), 231–250.

Blanchard-Wrigglesworth, E., Barthélemy, A., Chevallier, M., Cullather, R., Fuckar, N., Massonnet, F., et al. (2017). Multi-model seasonal forecast of Arctic sea-ice: Forecast uncertainty at pan-Arctic and regional scales. *Climate Dynamics*, *49*(4), 1399–1410.

Blanchard-Wrigglesworth, E., Bitz, C., & Holland, M. (2011). Influence of initial conditions and climate forcing on predicting Arctic sea ice. *Geophysical Research Letters*, *38*, L18503. https://doi.org/10.1029/2011GL048807

Blanchard-Wrigglesworth, E., & Bushuk, M. (2018). Robustness of Arctic sea-ice predictability in GCMs. *Climate Dynamics*, *52*, 5555–5566.

Blanchard-Wrigglesworth, E., Cullather, R., Wang, W., Zhang, J., & Bitz, C. (2015). Model forecast skill and sensitivity to initial conditions in the seasonal sea ice outlook. *Geophysical Research Letters*, *42*, 8042–8048. https://doi.org/10.1002/2015GL065860

Blockley, E. W., & Peterson, K. A. (2018). Improving Met Office seasonal predictions of Arctic sea ice using assimilation of CryoSat-2 thickness. *The Cryosphere*, *12*(11), 3419–3438.

Brunette, C., Tremblay, B., & Newton, R. (2019). Winter coastal divergence as a predictor for the minimum sea ice extent in the Laptev Sea. *Journal of Climate*, *32*, 1063–1080.

Bushuk, M., Msadek, R., Winton, M., Vecchi, G. A., Gudgel, R., Rosati, A., & Yang, X. (2017a). Skillful regional prediction of Arctic sea ice on seasonal timescales. *Geophysical Research Letters*, *44*, 4953–4964. https://doi.org/10.1002/2017GL073155

Bushuk, M., Msadek, R., Winton, M., Vecchi, G. A., Gudgel, R., Rosati, A., & Yang, X. (2017b). Summer enhancement of Arctic sea ice volume anomalies in the September-ice zone. *Journal of Climate*, *30*(7), 2341–2362.
Bushuk, M., Msadek, R., Winton, M., Vecchi, G., Yang, X., Rosati, A., & Gudgel, R. (2018). Regional Arctic sea–ice prediction: Potential versus operational seasonal forecast skill. *Climate Dynamics*, *52*, 2721–2743.
Cavalieri, D., & Parkinson, C. (2012). Arctic sea ice variability and trends, 1979–2010. *The Cryosphere*, *6*(4), 881–889.
Chevallier, M., Salas y Mélia, D., Voldoire, A., Déqué, M., & Garric, G. (2013). Seasonal forecasts of the pan-Arctic sea ice extent using a GCM-based seasonal prediction system. *Journal of Climate*, *26*(16), 6092–6104.
Chevallier, M., & Salas-Mélia, D. (2012). The role of sea ice thickness distribution in the Arctic sea ice potential predictability: A diagnostic approach with a coupled GCM. *Journal of Climate*, *25*(8), 3025–3038.
Collins, M. (2002). Climate predictability on interannual to decadal time scales: The initial value problem. *Climate Dynamics*, *19*(8), 671–692.
Collow, T. W., Wang, W., Kumar, A., & Zhang, J. (2015). Improving Arctic sea ice prediction using PIOMAS initial sea ice thickness in a coupled ocean–atmosphere model. *Monthly Weather Review*, *143*(11), 4618–4630.
Comiso, J. C. (2002). A rapidly declining perennial sea ice cover in the Arctic. *Geophysical Research Letters*, *29*(20), 1956. https://doi.org/10.1029/2002GL015650
Comiso, J. C., Parkinson, C. L., Gersten, R., & Stock, L. (2008). Accelerated decline in the Arctic sea ice cover. *Geophysical research letters*, *35*, L01703. https://doi.org/10.1029/2007GL031972
Day, J., Hawkins, E., & Tietsche, S. (2014). Will Arctic sea ice thickness initialization improve seasonal forecast skill? *Geophysical Research Letters*, *41*, 7566–7575. https://doi.org/10.1002/2014GL061694
Day, J. J., Tietsche, S., Collins, M., Goessling, H. F., Guemas, V., Guillory, A., et al. (2016). The Arctic predictability and prediction on seasonal-to-interannual timescales (apposite) data set version 1. *Geoscientific Model Development*, *9*, 2255–2270.
Day, J., Tietsche, S., & Hawkins, E. (2014). Pan-Arctic and regional sea ice predictability: Initialization month dependence. *Journal of Climate*, *27*(12), 4371–4390.
Dirkson, A., Merryfield, W. J., & Monahan, A. (2017). Impacts of sea ice thickness initialization on seasonal Arctic sea ice predictions. *Journal of Climate*, *30*(3), 1001–1017.
Eicken, H. (2013). Ocean science: Arctic sea ice needs better forecasts. *Nature*, *497*(7450), 431–433.
Ford, J. D., & Smit, B. (2004). A framework for assessing the vulnerability of communities in the Canadian Arctic to risks associated with climate change. *Arctic*, *57*, 389–400.
Germe, A., Chevallier, M., y Mélia, D. S., Sanchez-Gomez, E., & Cassou, C. (2014). Interannual predictability of Arctic sea ice in a global climate model: Regional contrasts and temporal evolution. *Climate Dynamics*, *43*(9-10), 2519–2538.
Guemas, V., Blanchard-Wrigglesworth, E., Chevallier, M., Day, J. J., Déqué, M., Doblas-Reyes, F. J., et al. (2016). A review on Arctic sea-ice predictability and prediction on seasonal to decadal time-scales. *Quarterly Journal of the Royal Meteorological Society*, *142*(695), 546–561.
Hansen, J., Ruedy, R., Sato, M., & Lo, K. (2010). Global surface temperature change. *Reviews of Geophysics*, *48*, RG4004. https://doi.org/10.1029/2010RG000345
Hofstra, N., Haylock, M., New, M., Jones, P., & Frei, C. (2008). Comparison of six methods for the interpolation of daily, European climate data. *Journal of Geophysical Research*, *113*, D21110. https://doi.org/10.1029/2008JD010100
Holland, M. M., Bailey, D. A., & Vavrus, S. (2011). Inherent sea ice predictability in the rapidly changing Arctic environment of the community climate system model, version 3. *Climate Dynamics*, *36*(7-8), 1239–1253.
Holland, M. M., & Stroeve, J. (2011). Changing seasonal sea ice predictor relationships in a changing Arctic climate. *Geophysical Research Letters*, *38*, L18501. https://doi.org/10.1029/2011GL049303
Johannessen, O. M., Shalina, E. V., & Miles, M. W. (1999). Satellite evidence for an Arctic sea ice cover in transformation. *Science*, *286*(5446), 1937–1939.
Jung, T., Gordon, N. D., Bauer, P., Bromwich, D. H., Chevallier, M., Day, J. J., et al. (2016). Advancing polar prediction capabilities on daily to seasonal time scales. *Bulletin of the American Meteorological Society*, *97*(9), 1631–1647.
Koenigk, T., & Mikolajewicz, U. (2009). Seasonal to interannual climate predictability in mid and high northern latitudes in a global coupled model. *Climate Dynamics*, *32*(6), 783.
Krikken, F., Schmeits, M., Vlot, W., Guemas, V., & Hazeleger, W. (2016). Skill improvement of dynamical seasonal Arctic sea ice forecasts. *Geophysical Research Letters*, *43*, 5124–5132. https://doi.org/10.1002/2016GL068462
Kwok, R., & Rothrock, D. (2009). Decline in Arctic sea ice thickness from submarine and ICESat records: 1958–2008. *Geophysical Research Letters*, *36*, L15501. https://doi.org/10.1029/2009GL039035
Laliberté, F, Howell, S., & Kushner, P. J. (2016). Regional variability of a projected sea ice-free Arctic during the summer months. *Geophysical Research Letters*, *43*, 256–263. https://doi.org/10.1002/2015GL066855
Lindsay, R., Zhang, J., Schweiger, A., & Steele, M. (2008). Seasonal predictions of ice extent in the Arctic Ocean. *Journal of Geophysical Research*, *113*, C02023. https://doi.org/10.1029/2007JC004259
Maslanik, J., Stroeve, J., Fowler, C., & Emery, W. (2011). Distribution and trends in Arctic sea ice age through spring 2011. *Geophysical Research Letters*, *38*, L13502. https://doi.org/10.1029/2011GL047735
Massonnet, F., Fichefet, T., Goosse, H., Bitz, C. M., Philippon-Berthier, G., Holland, M. M., & Barriat, P.-Y. (2012). Constraining projections of summer Arctic sea ice. *The Cryosphere*, *6*(6), 1383–1394.
Melia, N., Haines, K., & Hawkins, E. (2016). Sea ice decline and 21st century trans-Arctic shipping routes. *Geophysical Research Letters*, *43*, 9720–9728. https://doi.org/10.1002/2016GL069315
Meng, X.-L., Rosenthal, R., & Rubin, D. B. (1992). Comparing correlated correlation coefficients. *Psychological Bulletin*, *111*(1), 172–175.
Merryfield, W., Lee, W.-S., Wang, W., Chen, M., & Kumar, A. (2013). Multi-system seasonal predictions of Arctic sea ice. *Geophysical Research Letters*, *40*, 1551–1556. https://doi.org/10.1002/grl.50317
Mortin, J., Svensson, G., Graversen, R. G., Kapsch, M.-L., Stroeve, J. C., & Boisvert, L. N. (2016). Melt onset over Arctic sea ice controlled by atmospheric moisture transport. *Geophysical Research Letters*, *43*, 6636–6642. https://doi.org/10.1002/2016GL069330
Msadek, R., Vecchi, G., Winton, M., & Gudgel, R. (2014). Importance of initial conditions in seasonal predictions of Arctic sea ice extent. *Geophysical Research Letters*, *41*, 5208–5215. https://doi.org/10.1002/2014GL060799
Ordoñez, A. C., Bitz, C. M., & Blanchard-Wrigglesworth, E. (2018). Processes controlling Arctic and Antarctic sea ice predictability in the Community Earth System Model. *Journal of Climate*, *31*(23), 9771–9786.
Parkinson, C. L., Cavalieri, D. J., Gloersen, P., Zwally, H. J., & Comiso, J. C. (1999). Arctic sea ice extents, areas, and trends, 1978–1996. *Journal of Geophysical Research*, *104*(C9), 20,837–20,856.
Perovich, D. K., & Polashenski, C. (2012). Albedo evolution of seasonal Arctic sea ice. *Geophysical Research Letters*, *39*, L08501. https://doi.org/10.1029/2012GL051432

Peterson, K., Arribas, A., Hewitt, H., Keen, A., Lea, D., & McLaren, A. (2015). Assessing the forecast skill of Arctic sea ice extent in the GloSea4 seasonal prediction system. *Climate Dynamics*, *44*(1-2), 147–162.
Petty, A., Schröder, D., Stroeve, J., Markus, T., Miller, J., Kurtz, N., et al. (2017). Skillful spring forecasts of September Arctic sea ice extent using passive microwave sea ice observations. *Earth's Future*, *5*, 254–263. https://doi.org/10.1002/2016EF000495
Pizzolato, L., Howell, S. E., Dawson, J., Laliberté, F., & Copland, L. (2016). The influence of declining sea ice on shipping activity in the Canadian Arctic. *Geophysical Research Letters*, *43*, 12,146–12,154. https://doi.org/10.1002/2016GL071489
Regehr, E. V., Lunn, N. J., Amstrup, S. C., & Stirling, I. (2007). Effects of earlier sea ice breakup on survival and population size of polar bears in Western Hudson Bay. *The Journal of Wildlife Management*, *71*(8), 2673–2683.
Ricker, R., Hendricks, S., Helm, V., Skourup, H., & Davidson, M. (2014). Sensitivity of CryoSat-2 Arctic sea-ice freeboard and thickness on radar-waveform interpretation. *The Cryosphere*, *8*(4), 1607–1622.
Rigor, I. G., & Wallace, J. M. (2004). Variations in the age of Arctic sea-ice and summer sea-ice extent. *Geophysical Research Letters*, *31*, L09401. https://doi.org/10.1029/2004GL019492
Rothrock, D. A., Yu, Y., & Maykut, G. A. (1999). Thinning of the Arctic sea-ice cover. *Geophysical Research Letters*, *26*(23), 3469–3472.
Schröder, D., Feltham, D. L., Flocco, D., & Tsamados, M. (2014). September Arctic sea-ice minimum predicted by spring melt-pond fraction. *Nature Climate Change*, *4*(5), 353–357.
Serreze, M. C., Holland, M. M., & Stroeve, J. (2007). Perspectives on the Arctic's shrinking sea-ice cover. *Science*, *315*(5818), 1533–1536.
Sigmond, M., Fyfe, J., Flato, G., Kharin, V., & Merryfield, W. (2013). Seasonal forecast skill of Arctic sea ice area in a dynamical forecast system. *Geophysical Research Letters*, *40*, 529–534. https://doi.org/10.1002/grl.50129
Sigmond, M., Reader, M., Flato, G., Merryfield, W., & Tivy, A. (2016). Skillful seasonal forecasts of Arctic sea ice retreat and advance dates in a dynamical forecast system. *Geophysical Research Letters*, *43*, 12,457–12,465. https://doi.org/10.1002/2016GL071396
Smith, L. C., & Stephenson, S. R. (2013). New trans-Arctic shipping routes navigable by midcentury. *Proceedings of the National Academy of Sciences*, *110*(13), E1191–E1195.
Stroeve, J., Hamilton, L. C., Bitz, C. M., & Blanchard-Wrigglesworth, E. (2014). Predicting September sea ice: Ensemble skill of the search sea ice outlook 2008–2013. *Geophysical Research Letters*, *41*, 2411–2418. https://doi.org/10.1002/2014GL059388
Stroeve, J., Holland, M. M., Meier, W., Scambos, T., & Serreze, M. (2007). Arctic sea ice decline: Faster than forecast. *Geophysical research letters*, *34*, L09501. https://doi.org/10.1029/2007GL029703
Stroeve, J., Markus, T., Boisvert, L., Miller, J., & Barrett, A. (2014). Changes in Arctic melt season and implications for sea ice loss. *Geophysical Research Letters*, *41*, 1216–1225. https://doi.org/10.1002/2013GL058951
Taylor, K. E., Stouffer, R. J., & Meehl, G. A. (2012). An overview of CMIP5 and the experiment design. *Bulletin of the American Meteorological Society*, *93*(4), 485–498.
Tietsche, S., Day, J., Guemas, V., Hurlin, W., Keeley, S., Matei, D., et al. (2014). Seasonal to interannual Arctic sea ice predictability in current global climate models. *Geophysical Research Letters*, *41*, 1035–1043. https://doi.org/10.1002/2013GL058755
Tilling, R. L., Ridout, A., Shepherd, A., & Wingham, D. J. (2015). Increased Arctic sea ice volume after anomalously low melting in 2013. *Nature Geoscience*, *8*(8), 643–646.
Vecchi, G. A., Delworth, T., Gudgel, R., Kapnick, S., Rosati, A., Wittenberg, A. T., et al. (2014). On the seasonal forecasting of regional tropical cyclone activity. *Journal of Climate*, *27*(21), 7994–8016.
Wang, W., Chen, M., & Kumar, A. (2013). Seasonal prediction of Arctic sea ice extent from a coupled dynamical forecast system. *Monthly Weather Review*, *141*(4), 1375–1394.
Wang, L., Yuan, X., Ting, M., & Li, C. (2016). Predicting summer Arctic sea ice concentration intraseasonal variability using a vector autoregressive model. *Journal of Climate*, *29*(4), 1529–1543.
Williams, J., Tremblay, B., Newton, R., & Allard, R. (2016). Dynamic preconditioning of the minimum September sea-ice extent. *Journal of Climate*, *29*(16), 5879–5891.
Wyllie-Echeverria, T., & Wooster, W. S. (1998). Year-to-year variations in bering sea ice cover and some consequences for fish distributions. *Fisheries Oceanography*, *7*(2), 159–170.
Yuan, X., Chen, D., Li, C., Wang, L., & Wang, W. (2016). Arctic sea ice seasonal prediction by a linear Markov model. *Journal of Climate*, *29*(22), 8151–8173.